ASSESSMENT OF CFD SIMULATION DATA APPLICABILITY FOR AERODYNAMIC LOADS ESTIMATION

Petr Doupník
Brno University of Technology
Technická 2896/2
616 69 Brno
Czech Republic
doupnik@fme.vutbr.cz

František Vaněk
Brno University of Technology
Technická 2896/2
616 69 Brno
Czech Republic
vanek@fme.vutbr.cz

Abstract. CFD analysis data were assessed as another verification instrument for the analytical approaches of aerostatic loads estimation. Important influence of the interference effects between fuselage, wing and engine nacelles of twin-turboprop aircraft was included in computational model.

Keywords. CFD, wing-fuselage, loads.

1 Introduction

Series of methods is adequate for the wing aerodynamic loads calculation with interference effects between wing and fuselage. It can be for example the empirical method well known as “NP-CAGI” method [1], further methods based on the modification of lifting line theory, panel methods and finally CFD (RANS) methods. CFD methods give likely the most complex information about the problem, but “this is only the simulation”. CFD results must be interpreted all the time carefully and it is necessary to compare CFD results to wind tunnel and flight test.

2 CFD analysis

Symmetry cases were solved for the wide range of velocities (190 to 390 km/h) and angles of attack (-8,0° to 13,7°) for the wing-fuselage-nacelles configuration and isolated wing. The hybrid unstructured meshes were prepared in the ANSYS ICEM CFD 12.1 software. Domain was bounded by hemisphere with the pressure-far-field boundary condition. The pressure-outlet boundary condition was defined for the engine air entry. The thin disk was used for the propeller flow simulation. The flow boundary condition was assigned for the originated volume with the source-term momentum. Momentum values corresponded to the propeller axial velocity profile for the given flight regime. Radial velocities were not defined. Therefore no propeller slipstream swirl was made. The CFD software Fluent 12.1 was used for computations. The implicit solver was chosen, the compressible flow with the Spalart-Allmaras turbulence model was simulated.

3 Integral results

Integral force quantities were obtained directly from Fluent for every part of aircraft like wing, fuselage, engine and landing gear nacelles and end tanks, see Fig. 1. The comparison of lift curves for the isolated wing, wing-fuselage-nacelle configuration and whole aircraft is showed in Fig. 2. The isolated wing and wing-fuselage-nacelle configuration lift curves are from CFD results. The whole aircraft lift curve is from the actual aerodynamic data sheet of solved airplane. The comparison shows the certain agreement of CFD and analytical data, however analytical lift curve of the wing-fuselage-nacelle configuration was not obtainable for the better comparison.

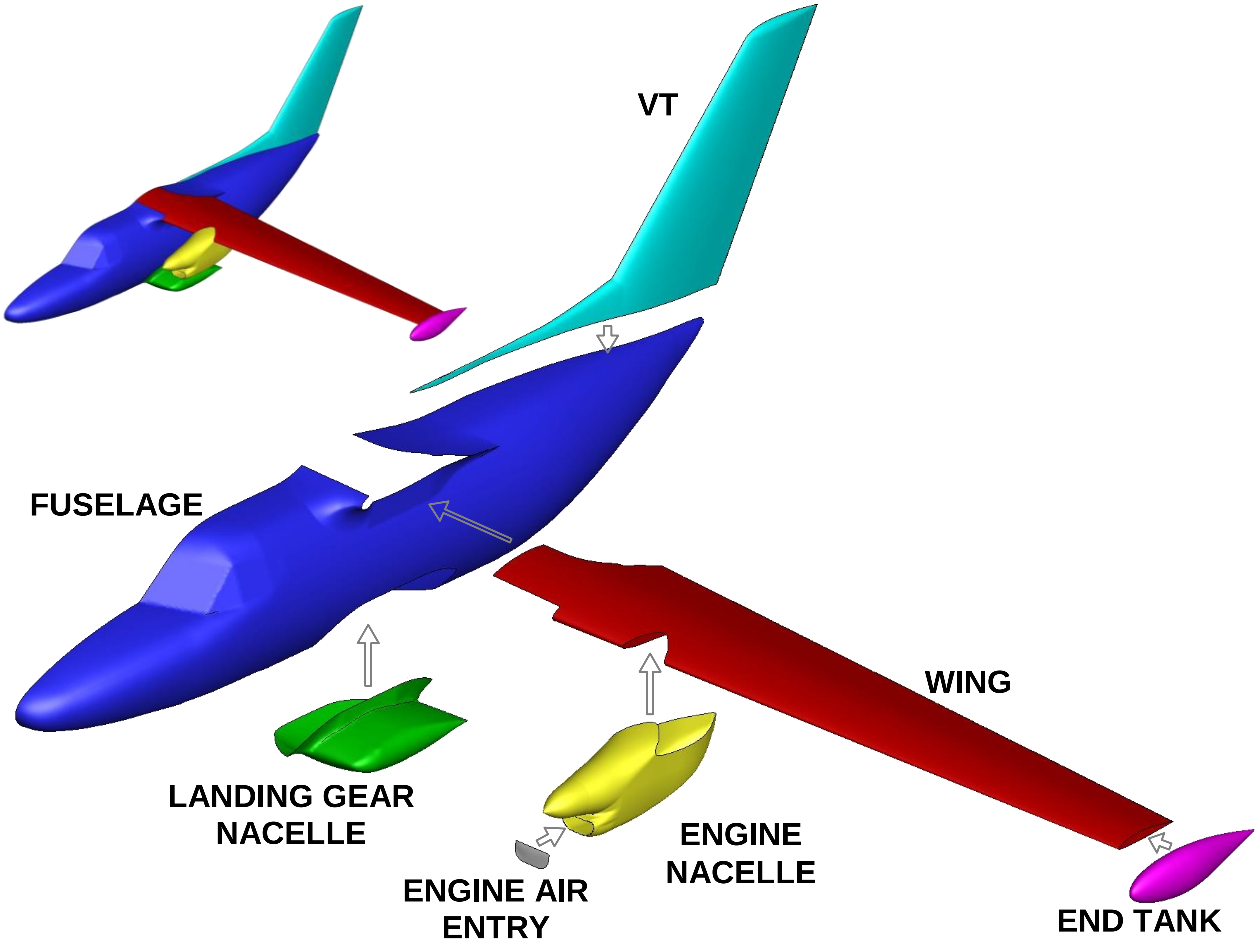

Figure 1: Parts of the 3D model.

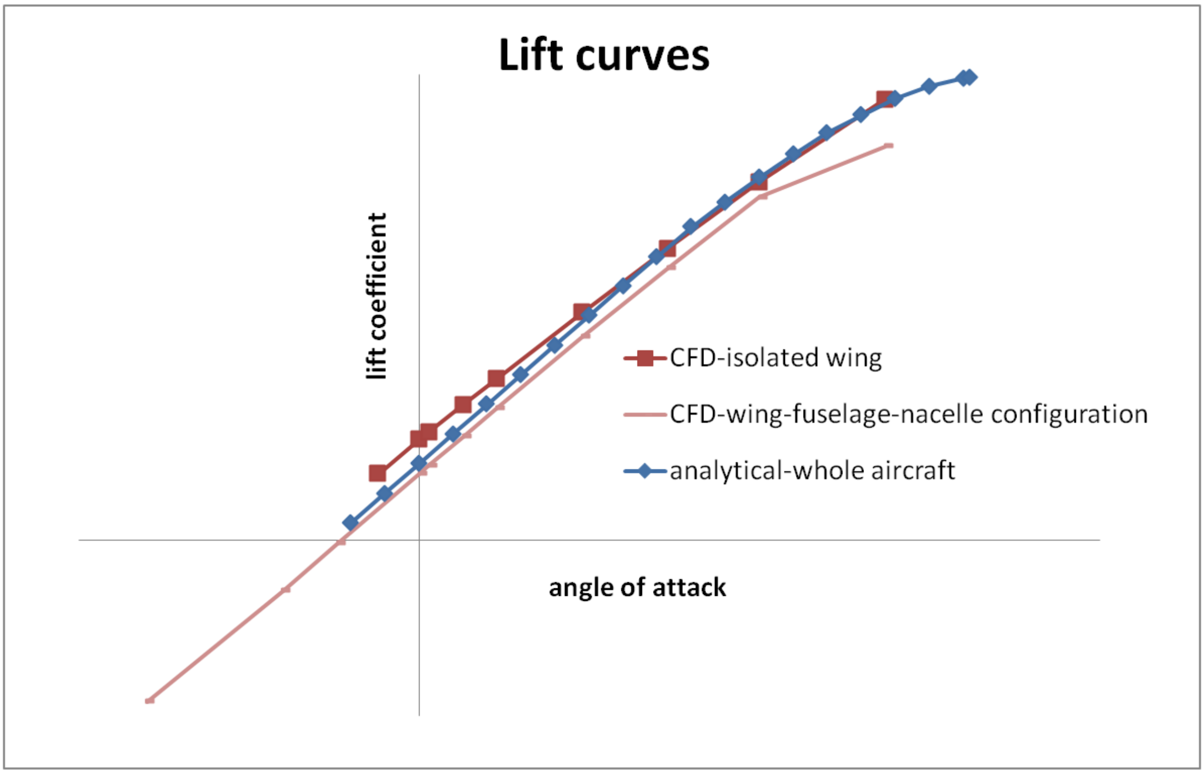

Figure 2: Comparison of the integral results.

4 Technique of work with CFD analysis results for the lift distribution

The surface pressure distribution from CFD results was for each case and each part exported to standard CFD postprocessor Tecplot format. Parts were divided in control slices; see Fig. 3, 4, 5. At these slices local lift and drag were integrated using in-house developed code. The lift distribution for the engine nacelle and end tank was corrected according to the lift coefficient from the Fluent software, because the number of control slice for this part was small. The lift distribution in the intersection of wing and engine nacelle was superposed by lift distribution of these parts. The intersection of wing and fuselage was solved similarly. The “NP-CAGI” principle was used for this problem, and this is, the total lift of fuselage (including fuselage, landing gear nacelle and vertical tail lift) is displaced on the wing (more precisely on wing-fuselage intersection). This matches to principle “zero fuselage influence”. Then the total lift of aircraft is wing lift plus horizontal tail lift. This is very good principle for the total equilibrium of aircraft, but slightly problematic for forces in the wing-fuselage connection, because forces are implemented into places, where they are not acting in fact. Consequently, the fuselage influence to the wing lift distribution was determined by the following way. The fuselage lift (including fuselage, landing gear nacelle and vertical tail lift) was lumped to the wing and subsequently this product was expanded to the corresponding wing part. Then, this “fuselage” lift distribution was added to the wing lift distribution.

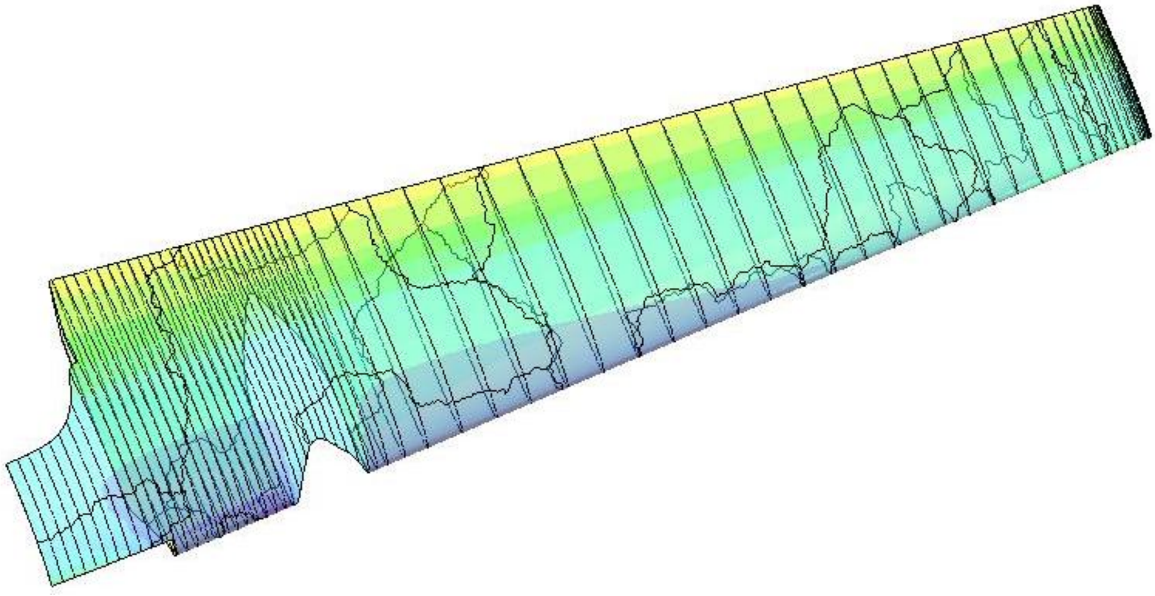

Figure 3: Wing control slices.

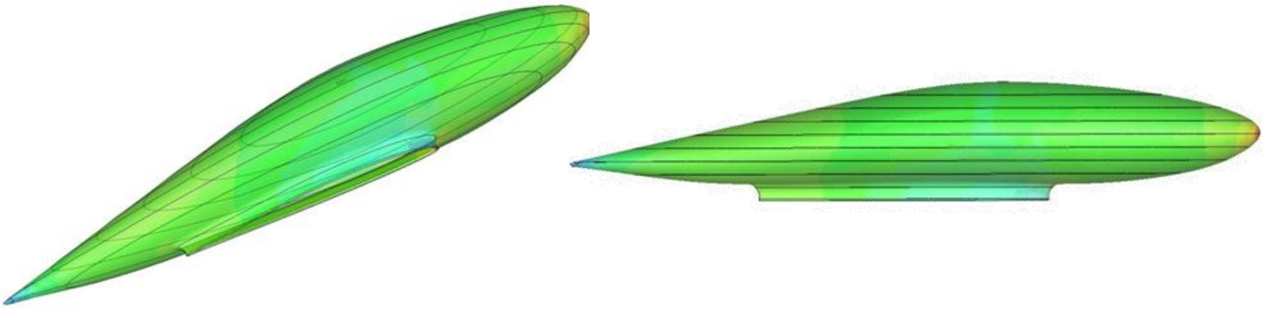

Figure 4: End tank control slices.

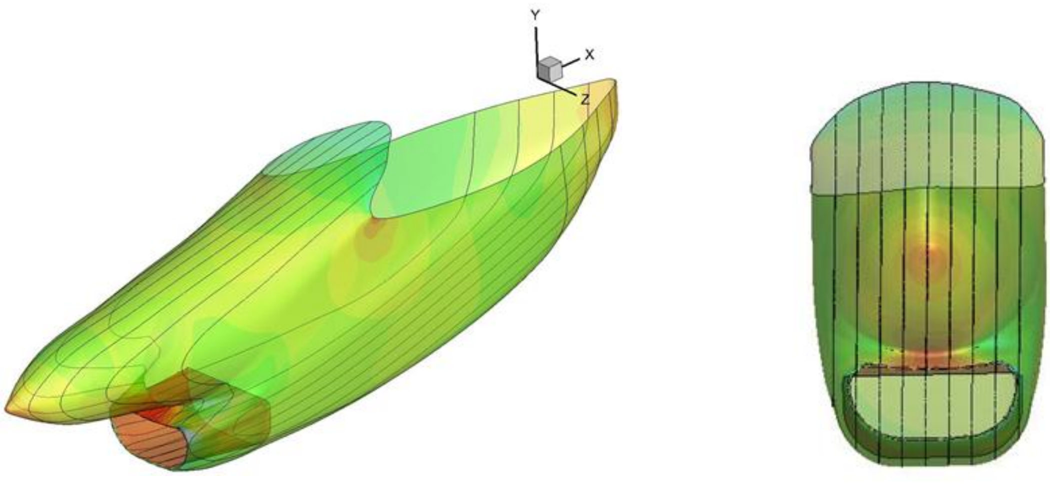

Figure 5: Engine nacelle control slices.

5 Isolated wing results

The CFD wing lift distribution for the isolated wing was compared with the analytical wing lift distribution from the earlier aerodynamic data sheets of solved airplane. This analytical lift distribution was made by way of classical lifting line theory (probably Multhop´s solution), with the correction to the end plates effect, by means of substitute extended wing and cutting off of the lift distribution.

The comparison of CFD and analytical distribution showed very good agreement, see Fig. 6. Force and moment distributions in large portion of wing were practically the same, in the wing root the values showed minimal differences; see Fig. 7, 8.

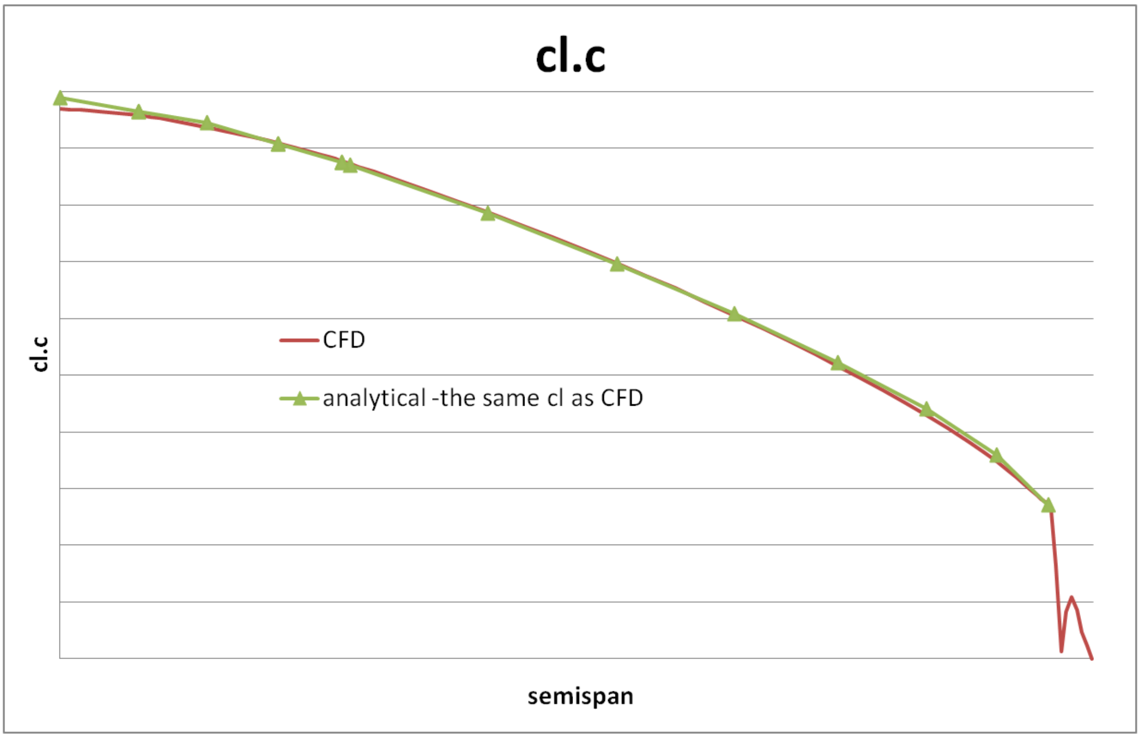

Figure 6: An example of the CFD and analytical lift distribution for the isolated wing.

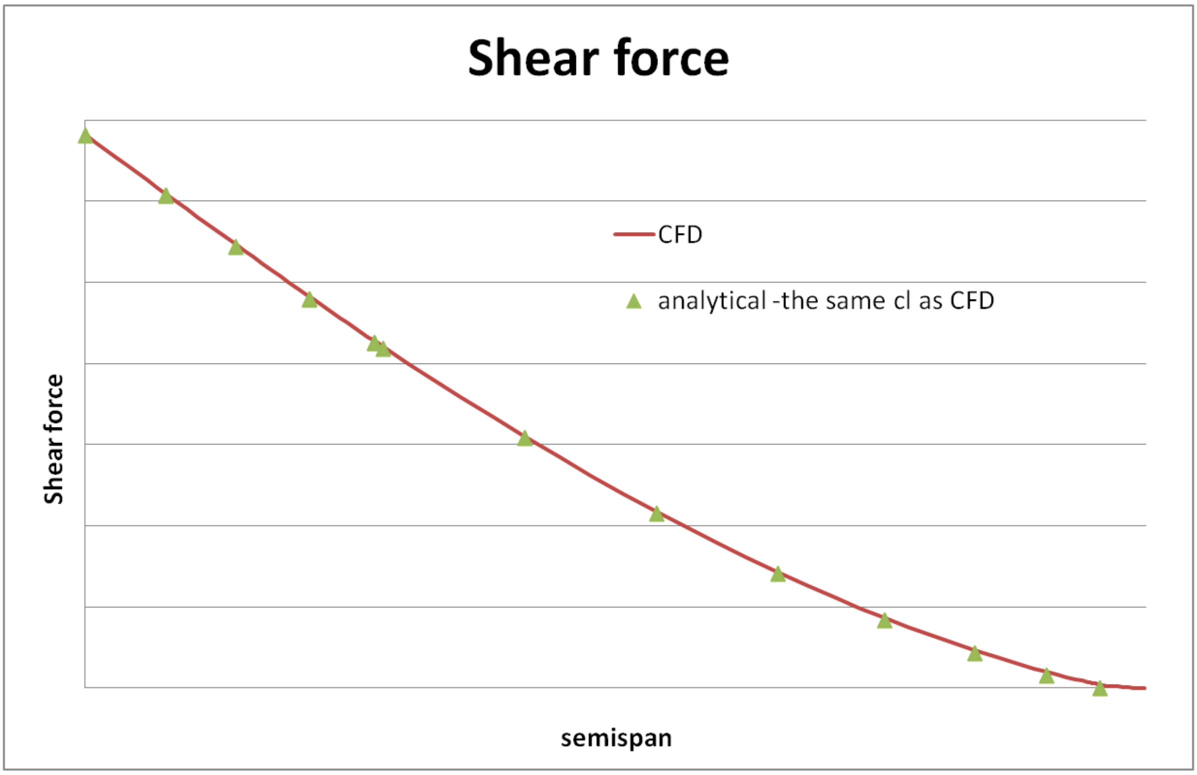

Figure 7: An example of the CFD and analytical shear force for the isolated wing.

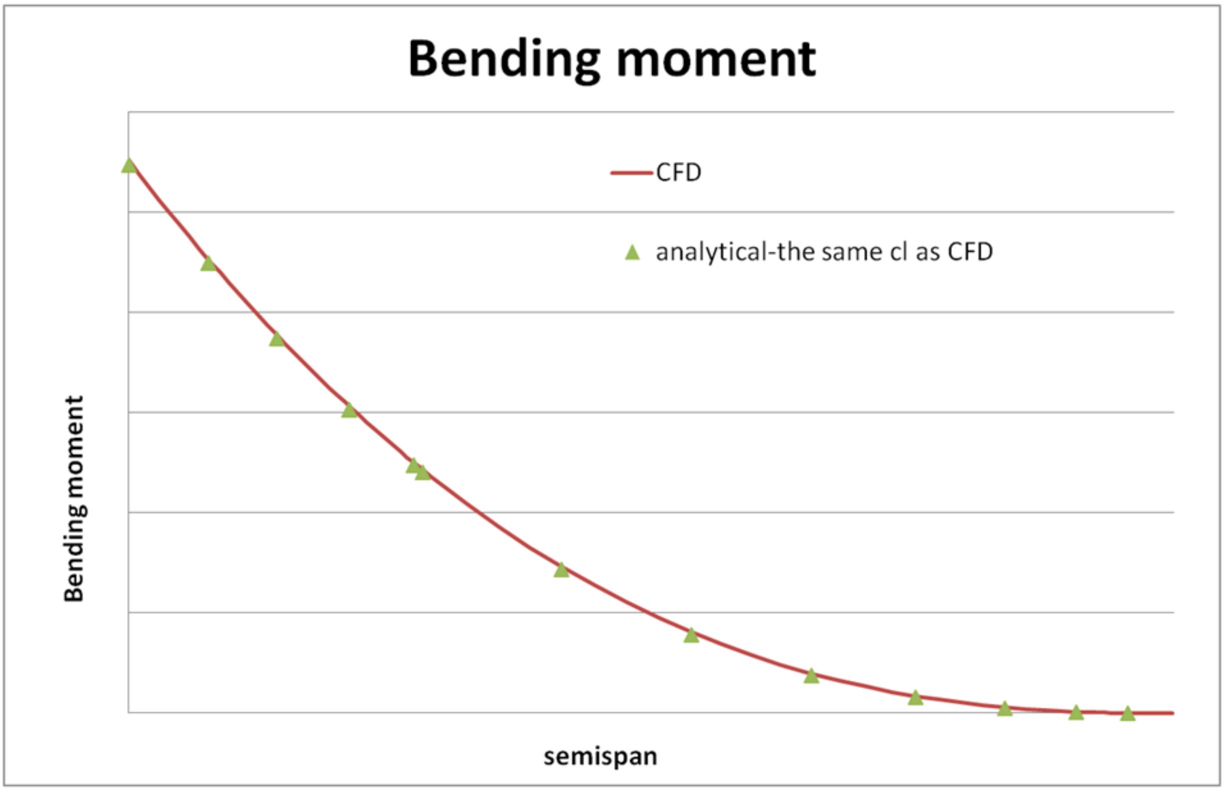

Figure 8: An example of the CFD and analytical bending moment for the isolated wing.

6 Wing-fuselage-nacelle configuration results

The CFD wing lift distribution for the wing-fuselage-nacelle configuration was compared with the analytical wing lift distribution from the earlier aerodynamic data sheets of solved airplane, too. This analytical lift distribution was made in accordance with the "NP-CAGI" method, where the unit basic (zero) distribution due to fuselage and engine nacelles for the dCLF = 1 (lift coefficient decrease due to fuselage and nacelles) is obtained from the additional (normal) lift distribution of isolated wing. This unit fuselage and nacelle distribution is multiplied by the corresponding dCLF for the required wing lift coefficient CLW. The dCLF - CLW dependence is possible to derive directly from the "NP-CAGI" method, or other proper way to use.

The comparison of CFD and analytical distribution showed acceptable agreement for middle and higher angles of attack; see Fig. 9. Force and moment distribution showed agreement for these angles of attack, too. The CFD and analytical distribution was different for small angles of attack. The higher lift decrease on wing-fuselage intersection and lift increase on outer wing was evident from CFD results in comparison with analytical method, see Fig. 10. Most probably, the influence of landing gear nacelle caused the big lift decrease on wing-fuselage intersection, because the landing gear nacelles generate strong negative lift on small angles of attack and this negative lift is part of the overall fuselage lift. Further, the CFD results did not show the same relative lift decrease on the fuselage and on the nacelle, which the "NP-CAGI" method assumes. CFD results disclaimed rather this assumed proportionality especially for small angles of attack.

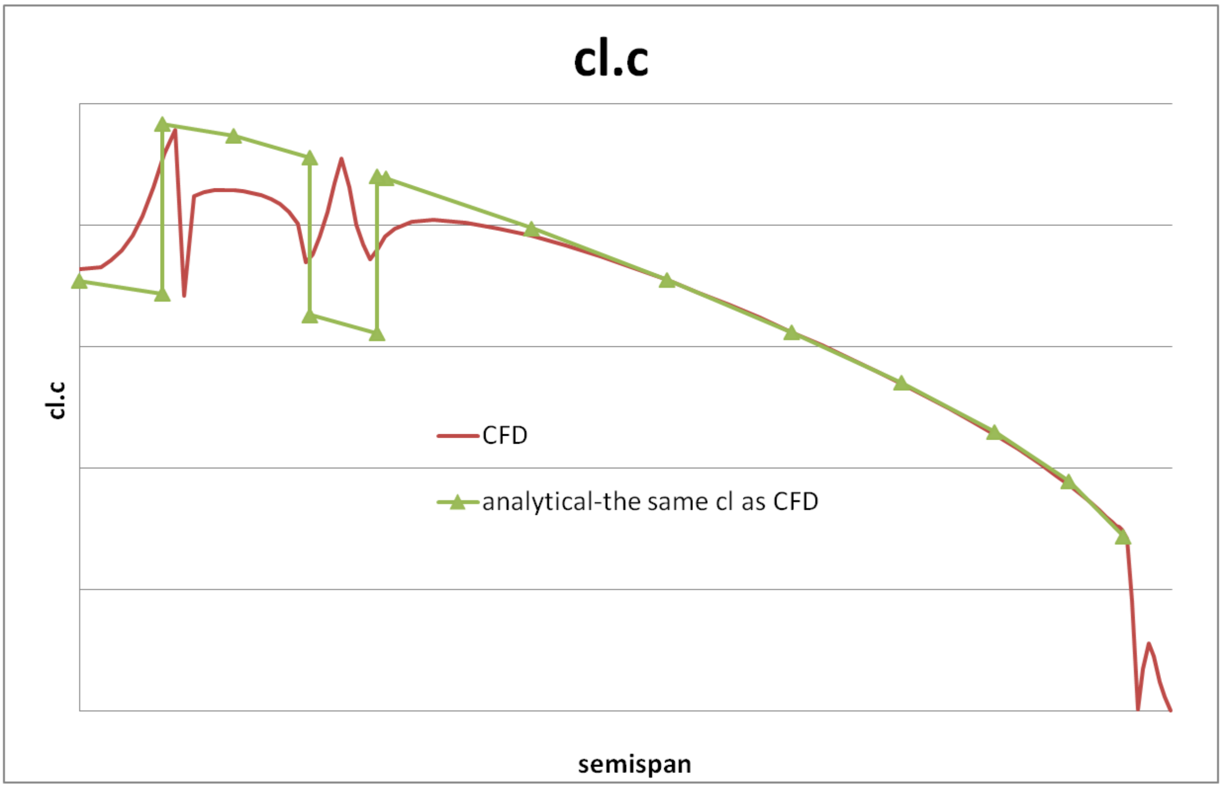

Figure 9: An example of the CFD and analytical lift distribution of the wing--fuselage-nacelle configuration for middle and higher angles of attack.

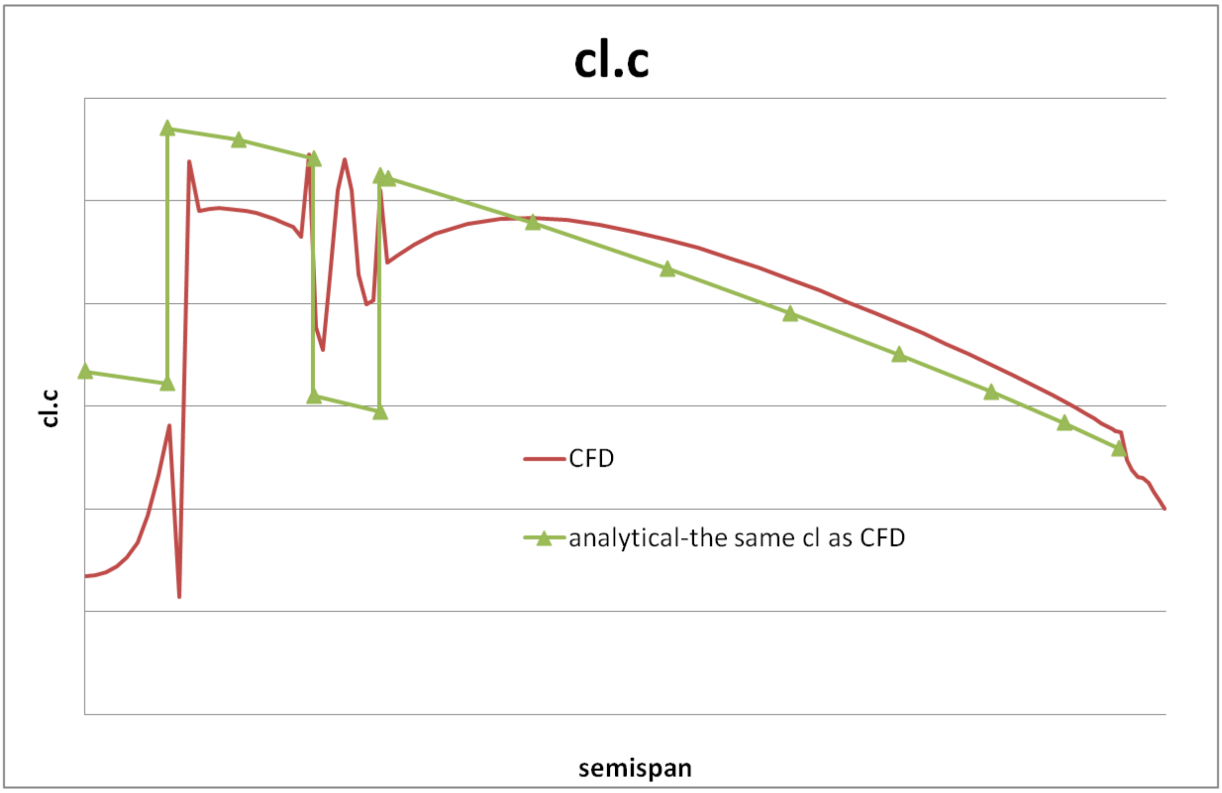

Figure 10: An example of the CFD and analytical lift distribution of the wing--fuselage-nacelle configuration for small angles of attack.

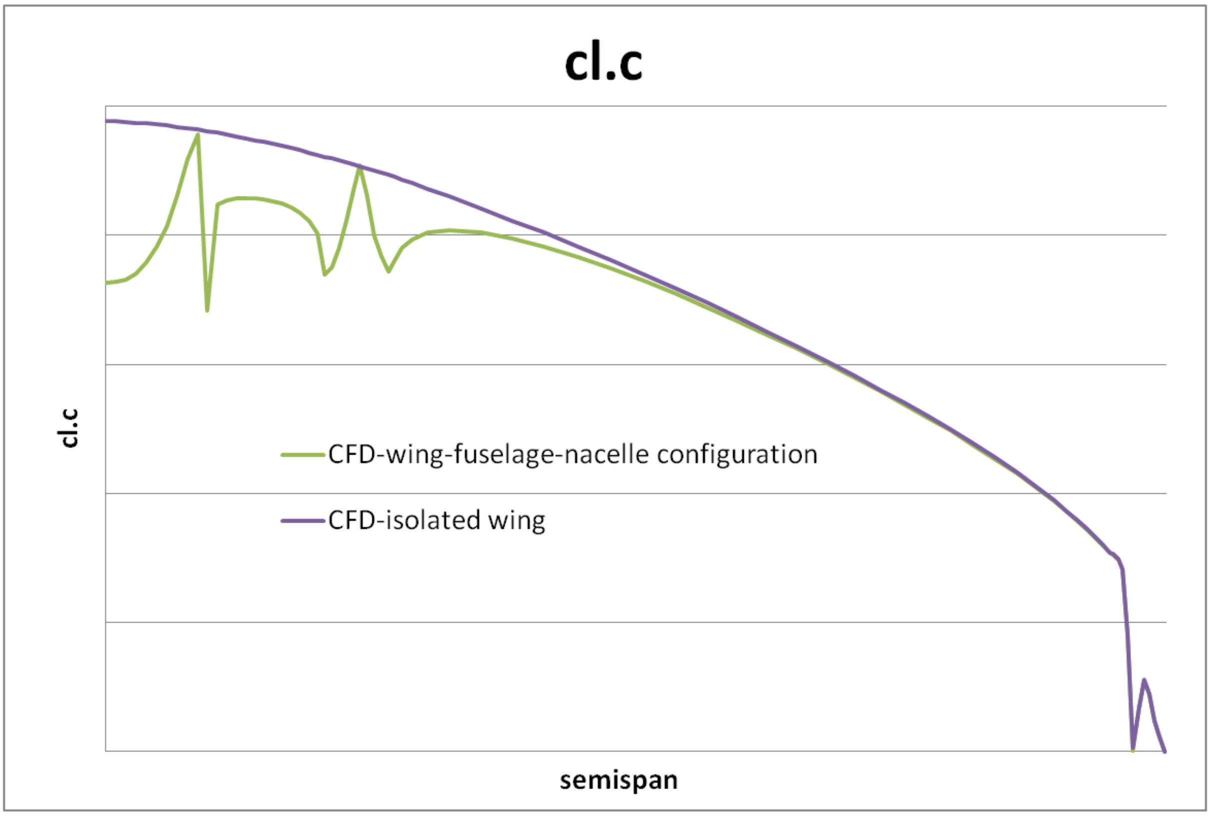

Figure 11: An example of the CFD lift distribution of the wing--fuselage-nacelle configuration and isolated wing for the same angle of attack.

7 Propeller flow influence

The comparison of CFD results with and without the propeller influence showed no propeller effect on the lift distribution of outer wing parts. The wing lift increase was visible in the propeller neighborhood. The engine nacelle showed the moderate lift decrease, the fuselage and landing gear nacelle on the contrary the moderate lift increase, see Fig. 12. The resultant lift dislocated thanks to lift redistribution inwards to the wing-span and the bending moment decreased.

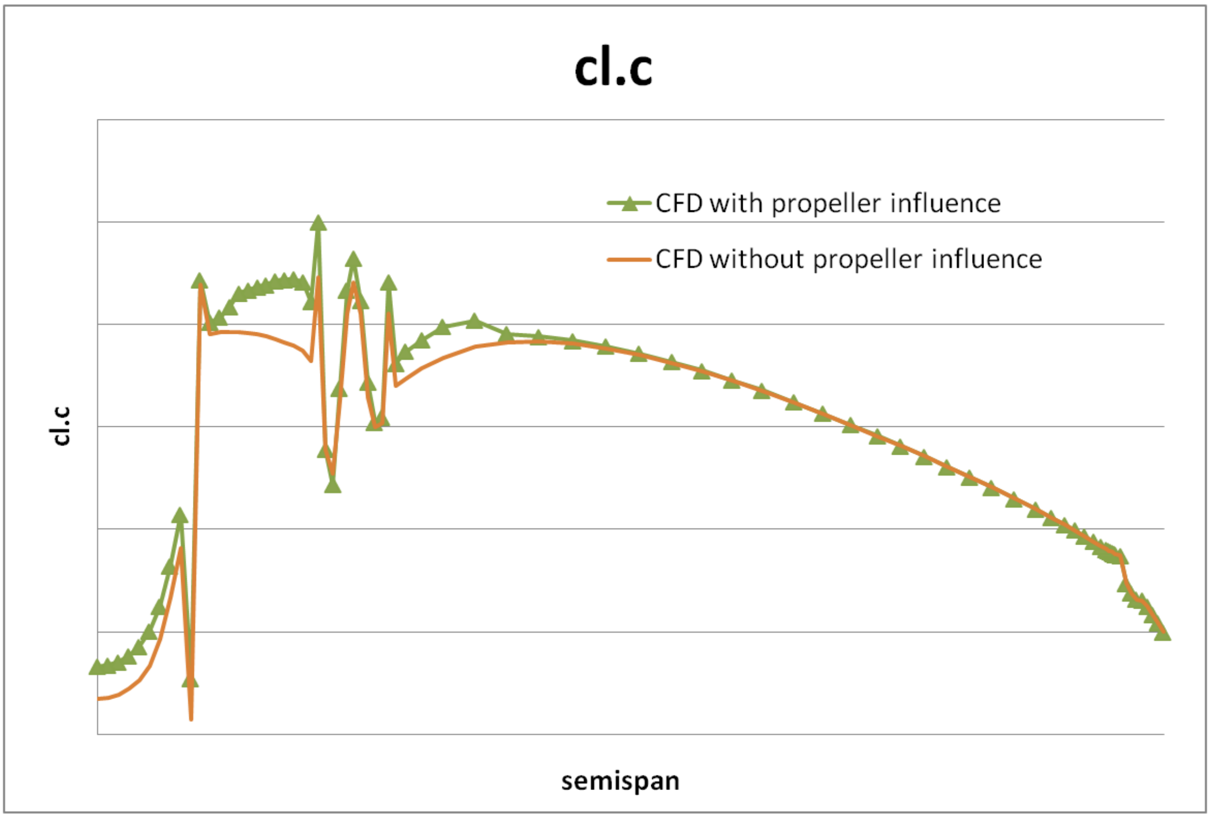

Figure 12: An example of the propeller flow influence for the wing--fuselage-nacelle configuration.

8 Conclusion

The realized CFD calculation of the aircraft without horizontal tail and of the isolated wing demonstrated possibilities of the determination of the CFD wing lift distribution, which is important primarily for the aircraft without horizontal tail. The CFD way allows describing of the character of the lift distribution with the fuselage influence for the real aircraft with its entire specialities considerably better, than common used analytical methods.

Acknowledgment

This project was realized with financial support of state budget by means of Ministry of Industry and Trade of Czech Republic under grant FR-TI2/557-Project MOSTA-Modernization of Small Transport Aircraft to increase operation effectiveness and economy.

References

[1] Russian regulation НП- ЦАГИ 1947.

[2] Vaněk, F., Kouřil, M. : The Aerodynamics Loads of the Wing-Winglet Configuration for UL and VLA Aircraft,, Czech aerospace proceedings/Letecký zpravodaj, Vol.2008, (2008), No.2, pp.30-34, ISSN 1211-877X, VZLU